

FATIGUE CRACK PROPAGATION FROM CRACK ARRAYS

W.J.D. Shaw* and I. Le May**

*Shaw Engineering & Research Corporation,
Saskatoon, Sask. Canada

**University of Saskatchewan,
Metallurgical Laboratory, Saskatoon, Sask. Canada

ABSTRACT

The prediction and measurement of fatigue crack propagation from crack arrays has been investigated. First, a K calibration curve was obtained for cracked, multiple edge notched (MEN) specimens and subsequently applied to determine the stress intensity factors. Second, an accurate data base for single edge notched (SEN) specimens was established in order to have a basis for comparison of the MEN fatigue crack growth data against those for single crack propagation. The results indicate that multiple cracks do not follow the same crack propagation law as do SEN cracks and exhibit different slopes of crack propagation rate versus ΔK . The extension of SEN analysis is insufficient to predict propagation of MEN cracks. Instabilities occur towards the later stages of MEN crack propagation and the specimen fails much more rapidly than expected. This characteristic of MEN specimens complicates the prediction of crack growth. Much work needs to be conducted into the propagation of MEN cracks prior to obtaining detailed laws for crack propagation and prediction of life.

KEYWORDS

Multiple crack propagation, fatigue crack propagation, crack arrays, array crack growth, crack growth prediction, multiple crack compliance, multiple crack instabilities, K calibration curves.

INTRODUCTION

Interest in the analysis and prediction of growth from fatigue crack arrays has arisen in recent years with the advent of high strength gun barrels. Multiple cracks form within the first few rounds when using these and a significant portion of their life is taken up by the propagation of these crack arrays. However, owing to the complexity of the problem very little progress has resulted in the understanding of the basic laws governing this type of crack propagation and in enabling accurate predictive methods to be employed.

A major problem lies in the obtaining of an accurate compliance function for the barrel geometry. The solution to this problem has been pursued by others with

some success (Goldthorpe, 1973, 1977; Baratta, 1979; Pu and Hussain, 1979), however the complexity of the barrel geometry, internal pressures acting on the surface, autofrettage of the barrels and change in curvature of the crack front as it propagates, all make the experimental measurement and further analysis of crack propagation difficult. Consequently, there is an absence of crack propagation data and fatigue analysis for gun barrel crack arrays.

It has been suggested (Goldthorpe, 1973, 1977; Ritter and de Morton, 1977) that the propagation of multiple cracks will follow the same law with the same constants as for single cracks in the same material so long as the correct value of stress intensity factor is used. This principle has generally been accepted although never proven. Also, it has been suggested (Ritter and de Morton, 1977; James and Anderson, 1969) that if the crack propagation rate for multiple cracked specimens is measured and compared with that for the single crack propagation, the K calibration curves can be determined for the former.

The approach taken in this work was to measure the fatigue crack propagation of single cracks and multiple crack arrays and to determine the stress intensity factors for the latter, and to this end a simpler and more familiar geometry was chosen. Using this simpler geometry which was more compatible with existing laboratory measurement techniques and analysis, a systematic approach to the fundamentals of multiple crack propagation was undertaken. First, an accurate compliance function is required in order to establish the stress intensity factor functions of the multiple cracks. Second, an accurate predictive analysis of a single fatigue crack is needed in order to have a base value for comparison. Third and finally, crack propagation measurements of the multiple cracks must be made, followed by analysis using all of the results acquired.

SPECIMEN CONFIGURATION AND MATERIAL

In order to eliminate some of the complex variables that occur in gun barrels, such as the complex stress distribution in thick walled cylinders, the effect of pressure acting on the crack surfaces, and the change in curvature of the crack front during fatigue, and also to enable accurate measurement of the crack length and to facilitate control over the lengths of the cracks within the array to allow for periodic adjustments, a long plate specimen was chosen. The configuration is shown in Fig. 1, for both SEN and MEN specimens.

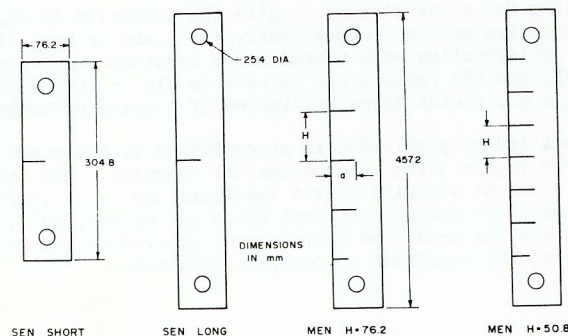


Fig. 1. Specimen configuration.

The use of edge notched specimens facilitated the adjustment of crack lengths for the MEN specimens by the use of special fixation clamps as shown in Fig. 2. These clamps restrained specific cracks from opening and closing, hence transferring the load across the crack away from the crack tip. This stopped the growth of the fixed crack. During the fatigue experiments this technique was applied as required to keep the multiple cracks at equal lengths (± 0.5 mm) so that the resultant stress intensity factor was within ± 0.1 MPa \sqrt{m} between adjacent cracks.

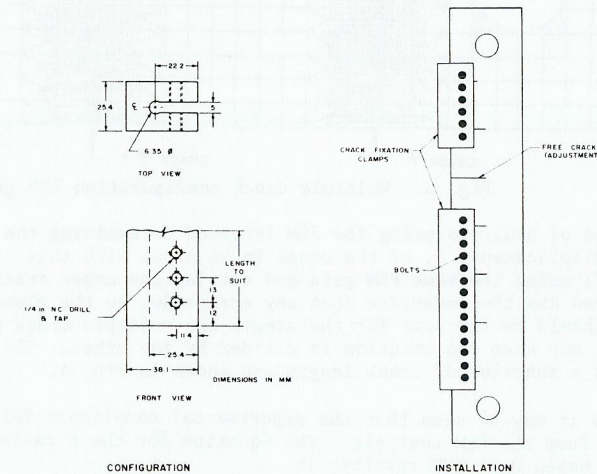


Fig. 2. Crack fixation clamps.

The material used was AISI 4140 steel, quenched and tempered at 300°C. The properties are given in Table 1.

TABLE 1 300°C Quenched & Tempered AISI 4140

Parameter	Value	Std Dev
Yield Strength	1677 \pm 10 MPa	
Ultimate Strength	1915 \pm 22 MPa	
Reduction in Area	24.6 \pm 2.5%	
Fracture Toughness	49.1 \pm 3.1 MPa \sqrt{m}	
Hardness	53.1 \pm 0.3 HRC	

This material is sensitive to environment, therefore all tests were conducted under controlled environmental conditions of 40% relative humidity and 22.2°C, with a loading frequency of 5 Hz (Shaw and Le May, 1976).

MULTIPLE CRACK COMPLIANCE

The compliance function of the finite width multiple crack specimens was obtained using two separate methods for the $H = 76.2$ mm specimens. The first involved the experimental determination of the compliance function and the second the use of the finite element method (FEM). The grid for the FEM is shown in Fig. 3. The compliance for the $H = 50.8$ mm specimen was determined experimentally, only. The measurement of displacement was along the load line.

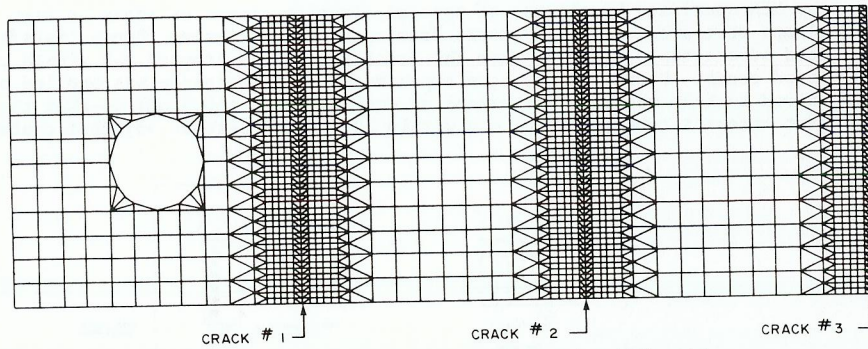


Fig. 3. Multiple crack configuration FEM grid.

The method of analysis using the FEM involved determining the ratio of crack opening displacement, δ , of the crack in an array with that of a single crack ($\delta_{MEN}/\delta_{SEN}$) using the same FEM grid and setting the other crack lengths to zero. This method has the advantage that any errors due to the element size and configuration should be the same for the single and multiple crack grids and hence tend to cancel out when one solution is divided by the other. The values of K calibration as a function of crack length are shown in Fig. 4.

From this it may be seen that the experimental compliance follows closely the value obtained from the FEM analysis. The equation for the K calibration curve for $H = 76.2$ mm, based upon FEM results, is

$$f(a/W) = 1.99 + 0.59(a/W) + 7.71(a/W)^2 - 6.67(a/W)^3 + 13.84(a/W)^4 \quad (1)$$

and should be accurate within 2%.

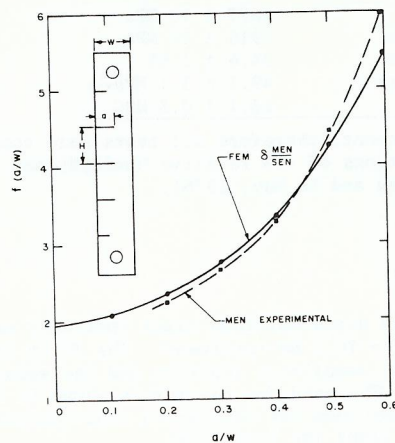


Fig. 4. MEN K calibration curves for $H = 76.2$ mm.

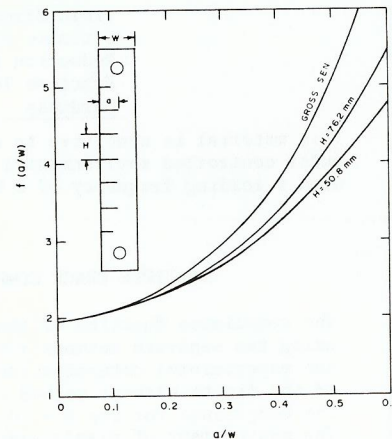


Fig. 5. MEN K calibration curves comparison.

The comparative K calibration curve for $H = 76.2$ mm, $H = 50.8$ mm and the SEN function are seen in Fig. 5.

The value of K calibration curve for the $H = 50.8$ mm spacing is

$$f(a/W) = 1.99 + 0.42(a/W) + 4.49(a/W)^2 + 8.49(a/W)^3 - 7.19(a/W)^4 \quad (2)$$

and is thought to be accurate to within 5%. A further check on the accuracy was conducted by analyzing photoelastic stress concentration data (Nishioka and Hisamitsu, 1962). At $a/W = 0.5$, agreement was found to be within 1.2% and at $a/W = 0.66$ to be within 9.3%. This approximate comparison gives good substantiation to the K calibration values for the MEN specimens shown in Fig. 5.

The stress intensity factor is now available for these two specimen configurations and can be calculated using the equation

$$K = \frac{P\alpha^{1/2}}{BW} f(a/W) \quad (3)$$

where P = applied load, B = specimen thickness and W = specimen width. The K calibration curve for the appropriate specimen can be substituted in Eq. (3).

SEN CRACK PREDICTION

The accuracy associated with the prediction of crack propagation of a single fatigue crack will determine the sensitivity with which the growth of multiple fatigue cracks can be compared and tested statistically. It is important to strive to reduce the statistical scatter and increase the accuracy of prediction to the greatest possible extent in order to make discriminating comparisons between SEN and MEN propagation data. For this reason techniques were used to reduce the scatter and increase the predictive accuracy to the greatest extent possible.

The techniques used, in addition to controlling the environment and geometric parameters, were the application of segmented fitting in lieu of overall fitting analysis, and taking crack closure into account. The method of segmented fitting is applied by breaking the crack growth curve up into four discrete segments over its entirety and fitting the Paris equation by least squares over each of these segments separately. The accuracy of this method over that of using the whole data region (overall fit) to fit the Paris equation is nearly an order of magnitude better. The use of this method has been documented (Shaw, 1979). Also, accounting for crack closure to give the effective ΔK has been shown to increase the predictive accuracy considerably (Shaw and Le May, 1979). Sixteen specimens of SEN configuration were tested under constant amplitude loading of 0.22 kN to 18.01 kN, and the results can be seen in Fig. 6, the abscissa showing normalized cycles, i.e., cycles after initiation of a crack of length $a = 16.51$ mm.

The crack growth prediction is accomplished by numerical integration over each segmented region using the appropriate equation. The statistical scatter is obtained from the analysis of the specimens and is an intrinsic value which depends only upon crack propagation rate (Shaw and Le May, 1977). It can be seen from Fig. 6 that the predicted curve almost duplicates the mean of the original data, indicating the excellent correlation obtained.

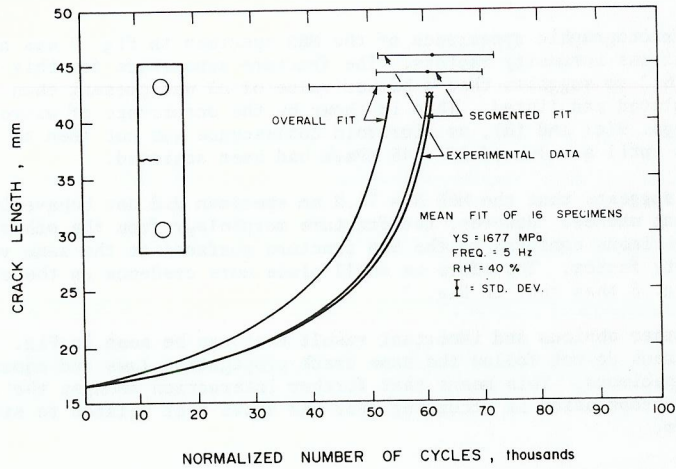


Fig. 6. SEN growth and prediction.

The analyzed data yielded four segmented fits as shown in Table 2.

TABLE 2 SEN Predictive Equations

Segment	ΔK Range	Equation
1	start - 25	$da/dN = 1.01717 \times 10^{-2} \Delta K^{3.4141}$
2	25 - 34	$da/dN = 2.7528 \times 10^{-2} \Delta K^{3.1037}$
3	34 - 44	$da/dN = 5.43122 \times 10^{-1} \Delta K^{2.2581}$
4	44 - failure	$da/dN = 0.1076 \Delta K$

da/dN - $\mu\text{m}/\text{cycle}$
 ΔK - $\text{MPa}\sqrt{\text{m}}$

MEN CRACK PROPAGATION

The data obtained in this portion of the program are of a preliminary nature since a limited number of specimens was used. One specimen was tested for $H = 76.2$ mm and two specimens for $H = 50.8$ mm. The actual and expected growth curves are shown in Figs. 7 and 8. The expected growth is based upon the SEN growth equations but using the MEN K calibration values, the curves being generated by numerical integration.

The growth curves for the MEN specimens were pieced together from the experimental data. The multiple crack lengths were adjusted by clamping from three to seven times during the life of the specimen, as required to maintain the length of the cracks within ± 0.5 mm tolerance of each other. The piecing together was done by extrapolating in both directions from the clamping period and calculating the number of cycles that would close the gaps between clamping periods. These adjustment periods represent less than 5% of the total life of the specimen and this technique should not result in serious inaccuracy to the overall growth curve.

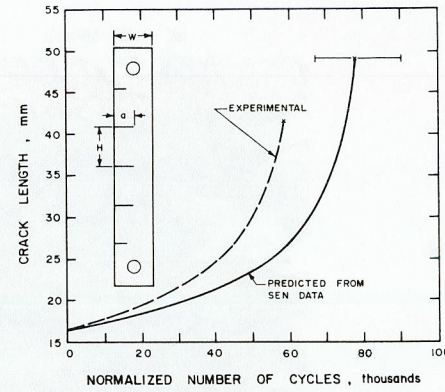


Fig. 7. MEN growth curve, $H = 76.2$ mm.

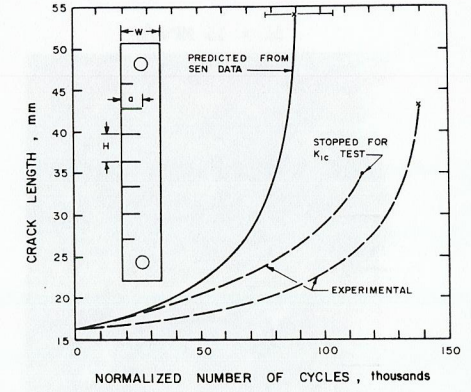


Fig. 8. MEN growth curve, $H = 50.8$ mm.

One test shown in Fig. 8 was stopped prior to failure and the middle crack was prepared for a fracture toughness test. The test results can be seen in Table 3: also compared are the values of stress intensity factor at fatigue fracture, K_{CF} , and the maximum value of K determined during K_{IC} testing, K_{CS} .

Note that Table 3 indicates that good correlation exists between the SEN specimens and the MEN specimen analyzed using the K calibration curve previously determined. The values for K_{IC} and K_{CS} indicate that the MEN failure condition is identical to that for the SEN specimens, being material dependent, as would be expected. However, the Table also indicates that under fatigue the final fracture values are not comparable to the SEN values, but lie between those for MEN specimens analyzed by MEN and SEN compliance procedures, being closer to the SEN analysis values. This is indicative of the instability occurring in the MEN specimens where the cracks stop growing in unison: one crack suddenly dominates and the stress intensity factor at the crack tip quickly approaches the SEN analysis values.

TABLE 3 MEN Fracture Toughness ($\text{MPa}\sqrt{\text{m}}$)

Mode	*SEN Values	MEN Analysis	SEN Analysis
K_{IC}	49.1 ± 3.1	45.14^+	55.91^+
K_{CS}	54.9 ± 3.9	52.08^+	64.51^+
K_{CF}	59.6 ± 3.6	$51.06\uparrow, 46.07\phi$	$64.35\phi, 64.65\phi$

* Mean of 16 specimens
 + MEN used for fracture toughness evaluation
 $\uparrow H = 76.2$ mm MEN
 $\phi H = 50.8$ mm MEN

As can be seen in Figs. 7 and 8 the final crack length at failure in the MEN specimens was considerably shorter than expected. This demonstrates the instability occurring in the experimental growth curves.

Examination of Figs. 7 and 8 indicates that the predicted and actual growth rates are at odds between the two graphs. Comparison of fractographic features of SEN and MEN specimens for comparable stress intensity factors (Fig. 9) indicates that

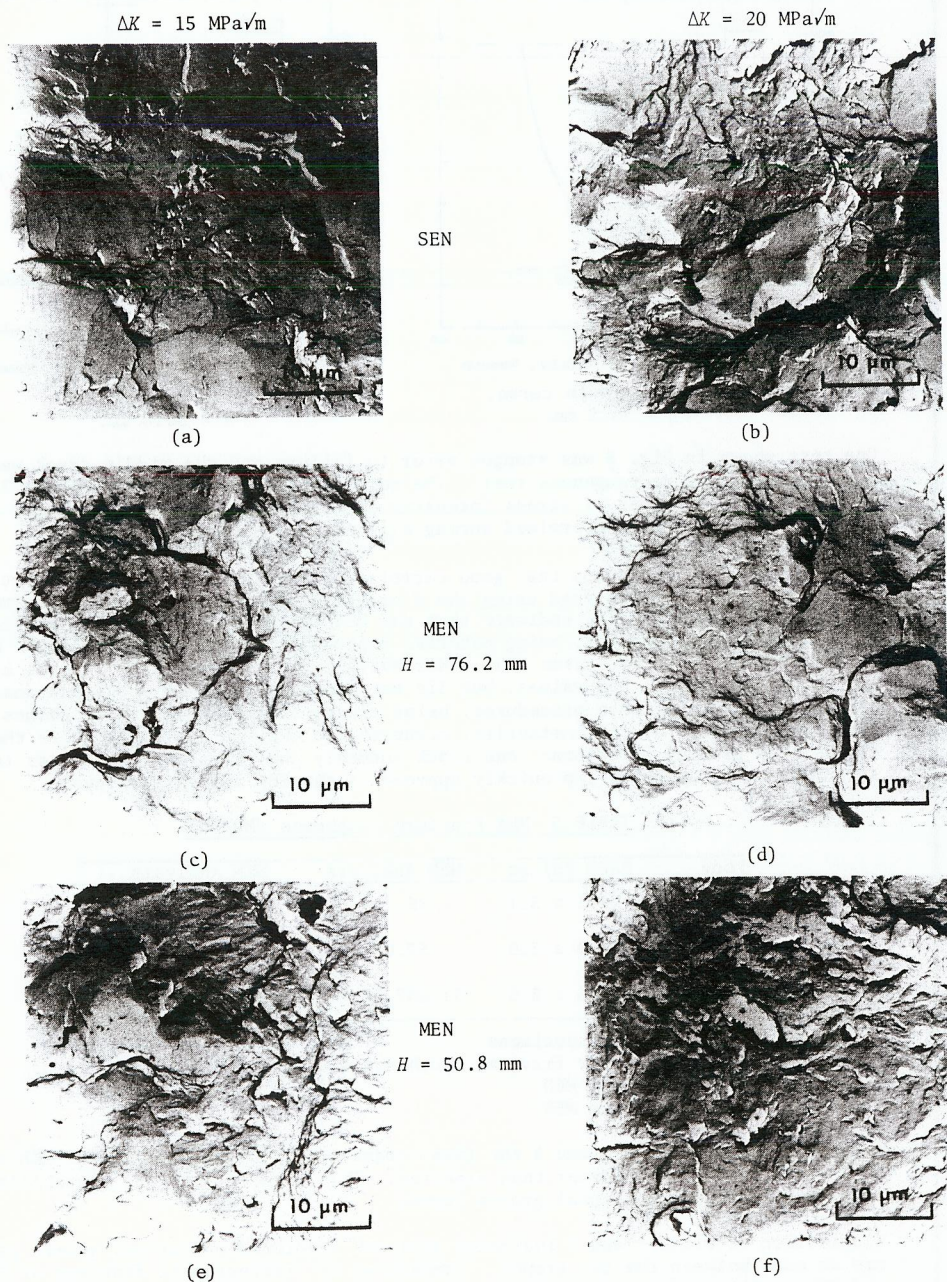


Fig. 9. Fractographic comparison of SEN and MEN specimens at two ΔK levels.

the fractographic appearance of the MEN specimen in Fig. 7 was not in keeping with the stress intensity factors. The fracture appearance for this MEN specimen with $H = 76.2$ mm suggests that a higher value of ΔK was present than that which was calculated and listed. This is shown by the occurrence of microvoid coalescence in Figs. 9(c) and (d), as microvoid coalescence was not seen to occur in SEN specimens until a value of $\Delta K = 45$ MPa \sqrt{m} had been achieved.

This suggests that the MEN $H = 76.2$ mm specimen did not behave in a normal or consistent manner. However, the fracture morphology from the other two MEN $H = 50.8$ mm specimens conforms to the SEN fracture surfaces at the same value of stress intensity factor. Therefore we shall place more credence on the experimental data of Fig. 8 than that in Fig. 7.

One other obvious and important result that can be seen in Fig. 8 is that the MEN specimens do not follow the same crack propagation laws and equations as do the SEN specimens. This means that further interaction amongst the cracks during fatigue propagation is occurring over and above that related to stress intensity factor.

DISCUSSION

Multiple fatigue crack propagation is extremely complex and considerable background work is required prior to conducting actual specimen tests. First the compliance function is required for the finite width or geometric specimen, which in itself is no small task. Second, a data base of constants and propagation laws of a single fatigue crack is required with as high an accuracy as possible. Third, the actual data for multiple cracks and their subsequent analysis need to be obtained. The amount of time and effort increases exponentially with the increase in the number of fatigue cracks present in one specimen. Thus it will not be an easy task to accumulate meaningful crack propagation data for multiple crack configurations.

The behavior of MEN cracks in the latter stages of propagation appears to indicate that a type of instability is occurring. Once a specific point has been reached the system exhibits an amplification effect hastening crack growth and shortening fatigue life to that expected from SEN prediction. It has been suggested that this phenomenon might occur in multiple crack problems (Goldthorpe, 1973, 1977).

It is also postulated that the difference in growth indicated between the MEN data and the predicted curves from SEN data results from an amplification of the erratic micro-growth pattern between different cracks (Lipsitt and co-workers, 1959) where only one crack grows periodically. Since there are a number of crack tips the energy available for crack propagation is dissipated unevenly between the different cracks. The multiple cracks tend to amplify this erratic growth pattern even further. Therefore it can be expected that a large statistical variation will occur during the propagation of multiple fatigue cracks as compared to that for a single propagating crack. This erratic growth behavior is probably the reason why the MEN cracks do not follow the same basic growth laws as do SEN cracks. Thus the extension of SEN data cannot be considered adequate nor representative in predicting multiple crack growth. Multiple cracks behave in the same way as single cracks when tested statically but yield differences when tested in the dynamic mode. The same erratic growth pattern and instability has been noted in the fatigue crack propagation of double edge notched specimens (Shaw, 1979).

The above work does not show conclusively that multiple cracks behave in a different manner from the propagation of a single crack. However, considering the results it would appear that the extension of SEN data is insufficient in predicting the behavior of multiple cracks. Further substantiation and verification are required before the results given can be taken as conclusive.

CONCLUSIONS

The following conclusions may be drawn:

1. The K calibration curves for two MEN configurations have been evaluated.
2. A data base of crack propagation equations for SEN specimens has been established.
3. Statically, MEN specimens and SEN specimens fracture at the same critical values of stress intensity factor.
4. Dynamically, MEN specimens deviate from the extension of SEN laws in:
 - a) propagation rate.
 - b) instabilities that occur in the latter stages of propagation.
5. The extension of SEN analysis to MEN specimens is not satisfactory.

ACKNOWLEDGEMENTS

The authors would like to acknowledge the financial support in the initial stages of the project from the Defence Research Board of Canada, Grant #7510-75, and the College of Graduate Studies, University of Saskatchewan, Grant #A-3064, for support in the latter stages of the work. Support from the Natural Sciences and Engineering Research Council of Canada is also gratefully acknowledged.

REFERENCES

- Baratta, F.I. (1978). *Eng. Fracture Mech.* 10, 691-697.
- Goldthorpe, B.D. (1973). Crack growth in pressurized thick-walled cylinders. In *Conference on Mechanics and Mechanisms of Crack Growth*. Churchill College, Cambridge. pp. 1-23.
- Goldthorpe, B.D. (1977). Fatigue and fracture of thick-walled cylinders and gun barrels. In T.P. Rich and D.J. Cartwright (Eds.), *Case Studies in Fracture Mechanics*. Army Materials and Mechanics Research Center, Watertown, Mass. pp. 3.8.1-3.8.15.
- James, L.A., and Anderson, W.E. (1969). *Eng. Fracture Mech.*, 1, 565-568.
- Lipsett, H.A., Forbes, F.W., and Baird, R.B. (1959). *Proc. ASTM*, 59, 734-747.
- Niskioka, K.U., and Hisamitsu, N. (1962). *Trans ASME, J. Appl. Mech.*, 29, 575-577.
- Pu, S.L., and Hussain, M.A. (1979). Stress intensity factor for a circular ring with a uniform array of radial cracks using cubic isoparametric singular elements. In C.W. Smith (Ed.), *Fracture Mechanics*, STP 677. ASTM, Philadelphia. pp. 685-699.
- Ritter, J.D., and de Morton, M.E. (1977). *J. Australas. Inst. Met.*, 22, 51-55.
- Shaw, W.J.D. (1979). *Fatigue Crack Propagation of Single Cracks and Multiple Crack Arrays in High Strength Steel*. Ph.D. Thesis. University of Saskatchewan.
- Shaw, W.J.D., and Le May, I. (1976). Fatigue crack propagation in high strength steel in controlled humidity conditions. In R.G. Bathgate (Ed.), *Fatigue Testing and Design*, Vol. 2. Soc. of Environmental Engineers, London, pp. 31.1-31.24.
- Shaw, W.J.D., and Le May, I. (1977). Fractographic studies and statistical scatter in fatigue crack propagation under controlled humidity conditions. In *The Influence of Environment on Fatigue*. I. Mech. E., London, pp. 93-100.
- Shaw, W.J.D., and Le May, I. (1979). Crack closure during fatigue crack propagation. In C.W. Smith (Ed.), *Fracture Mechanics*, STP 677. ASTM, Philadelphia. pp. 233-246.